BLADE TIP RUBBING STRESS PREDICTION*

Gerald A. Brusher**, Gary A. Davis, and Daniel M. Shea

Rockwell International/Rocketdyne Division
Canoga Park, California

ABSTRACT

A linear analysis was performed to determine the dynamic response of a turbine blade to intermittent rubbing against a tip seal. The response analysis consisted of a parametric study where the rubbing friction force was assumed to vary as a half sine wave over a preselected contact arc. The length of the contact arc, as well as the pump speed, was varied to determine the effects of each. Results show that for a given contact arc there are distinct critical speeds at which the blade response becomes a maximum.

INTRODUCTION

Due to the requirement for high efficiency in modern turbomachinery, clearances between turbine blade tips and the turbine housing are desired to be as small as is practically possible. An opposing design requirement is that the clearances be large enough to prevent rubbing of the blade tips on the housing due to rotor flexibility. In practice, a compromise is reached, and a small amount of rubbing is tolerated. For example, in the Space Shuttle Main Engine (SSME) high pressure fuel turbopump (Fig. 1), the first-stage turbine blades experience light rubbing over approximately 20 to 30 degrees of arc. To minimize tip rubbing while keeping the clearances as small as possible, the turbine is mounted eccentrically in the pump housing. Under steady-state operation, sideloads created by the pumping action of the impellers move the rotor to the centered position and no rubbing occurs. During startup, however, the rotor blades contact the pump housing for a short period of time; this has been observed in the turbine hardware during posttest inspections of the tip seal area. A typical seal segment showing the light rub patterns is presented in Fig. 2.

The purpose of the analysis presented herein was to assess the effects of tip rubbing on the dynamic response of turbine blades. In particular, the turbine blades of the SSME high pressure fuel turbopump were analyzed as a representative case.

*Work reported herein was sponsored by NASA/Marshall Space Flight Center under Contract NAS8-36361

**Presently attending the University of Michigan.

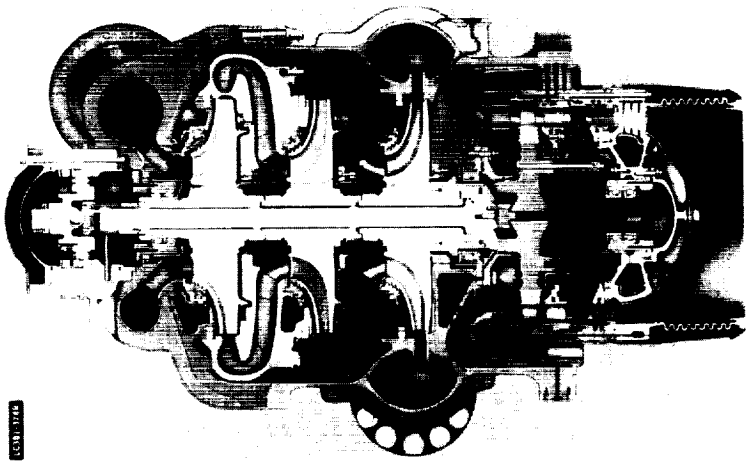

Fig. 1. High Pressure Fuel Turbopump

Fig. 2. HPFTP First-Stage Tip Seal Segment

ANALYTICAL MODEL

To investigate the problem of intermittent rubbing against a tip seal, an analytical model was developed that utilized a finite element representation of the turbine blade. The model (Fig. 3) addressed a single blade fixed at the shank root and free at the tip. The boundary conditions at the root simulate the fixity of the blade due to the centrifugal loads acting through the firtree during high speed operation. Since the flexibility of the disk actually admits motion of the blade shank, the assumption of fixity results in slight increases in both natural frequencies and stresses. However, these effects are inconsequential in regard to understanding the dynamic behavior of the blade due to to tip rubbing.

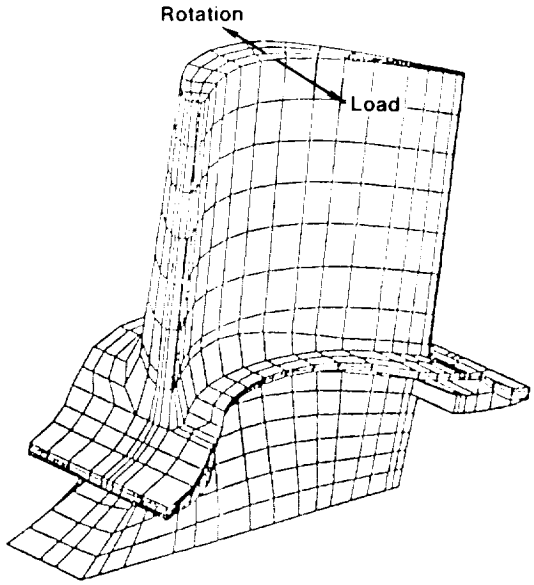

Fig. 3. HPFTP First-Stage Turbine Blade Finite Element Model

To represent the rotation of a rotor about an eccentric axis, it was assumed that the blade would be in contact with the tip seal over a well-defined arc once per revolution. Only tangential friction effects were considered; therefore, a tangential load was applied to a single point on blade tip. The amplitude of the forcing function was set equal to the product of the normal load and the friction coefficient. The friction coefficient was assumed to be constant, however, the normal load was assumed to vary as a half sine wave over the duration of the rub (Fig. 4). This assumption was reasonable given the kinematics of rotation about an eccentric axis.

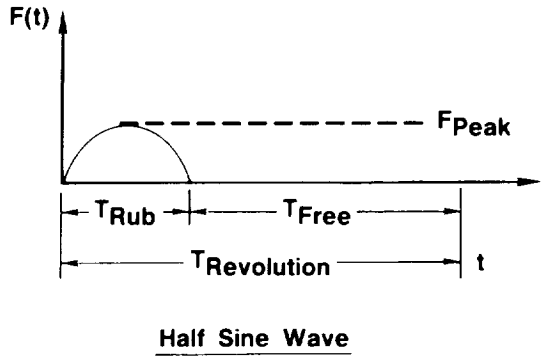

Fig. 4. Friction Force Time History

The model was designed to assess linear behavior only. It was initially postulated that the blade would display stick-slip behavior during contact with the seal. However, this was shown to be highly unlikely because the blade tip speed due to rotation is approximately 2000 times greater than that due to vibration in the first-tangential bending mode. Therefore, this nonlinearity was not included in the model.

METHOD OF SOLUTION

The modal analysis technique was used to solve the equations of motion for the blade. The first 10 natural frequencies and mode shapes were extracted from the finite element model and then used to express the uncoupled equations of motion in terms of principal coordinates. These uncoupled equations were solved through time integration using the central difference method. Modal displacements and stresses were then summed to compute the physical displacements and stresses at selected points on the blade.

PARAMETRIC ANALYSIS

Four parameters were expected to have a significant effect on the blade response: normal force, friction coefficient, shaft speed, and contact arc. Since it was difficult to specify exact values of these parameters, it was deemed preferable to determine the response over a range of values and then to rely on future empirical results to assist in pinpointing their actual magnitudes. Ranges for these parameters are presented in Table 1 and reflect experience with dynamic simulations of the rotor as well as known operational parameters of the pump.

A typical response analysis consisted of calculation of the steady-state solution for a specific normal force, friction coefficient, contact arc, turbine speed, and point of application of the rubbing force. The linear nature of the analysis was used as much as possible

Table 1. Parametric Analysis

Parameter	Minimum	Maximum	Increment
Normal Force (lb)	0	200	50
Friction Coefficient	0.1	0.3	0.1
Shaft Speed (rpm)	28,000	38,000	500
Contact Arc (deg)	10	30	10

to reduce the number of cases run. For example, the response results for a given friction coefficient and normal force were linearly scaled to different values of friction coefficient and normal force. The sensitivity of the response to the point of application of the load was investigated by forcing the blade tip near the center of the airfoil, the leading edge, and trailing edge. Finally, turbine speed and contact arc were varied by changing the frequency and shape of the forcing function.

DISCUSSION OF RESULTS

The most significant results obtained from the linear parametric analysis were the discoveries of critical speeds and contact arcs that maximized the response of the blade. In addition, it was found that regardless of whether the tangential friction force was applied to the blade tip near the center of the airfoil, or at the leading or trailing edge, the blade primarily responded in the lowest bending mode. Before discussing the causes for the occurrence of critical speeds and contact arcs, it will be instructive to consider the general aspects of the blade behavior in the time domain. Then the problem will be characterized in the frequency domain, yielding further insight into the response.

To begin, consider the behavior of a single blade as it moves through several revolutions of the turbine disk. This is shown in Fig. 5, which illustrates a typical time history of stress in the root region of the blade. The time between peak stresses corresponds to one revolution of the disk. For a given revolution, the maximum stress occurs at the end of the contact arc because the friction load causes the blade to deflect. At the end of the contact interval, the blade is released and then it experiences free, damped vibration for the remainder of the revolution. As can be seen from the Fig. 5, the blade response during the time of free vibration is a function of the damping ratio which was chosen as $\zeta = 0.01$ throughout this analysis. An alternate method of showing the motion is with a state space plot of the blade tip displacement as presented in Fig. 6. This graph, which is plotted for a single revolution of the turbine, clearly shows the disturbance from equilibrium due to rubbing and the subsequent damped response.

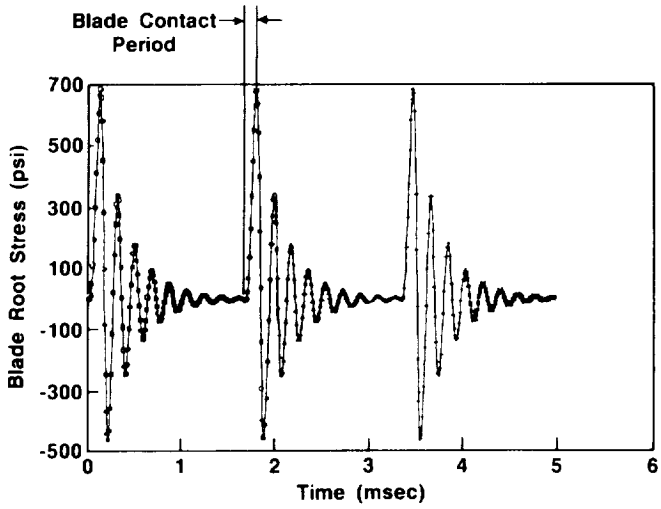

Fig. 5. Typical Stress Time History (Pump Speed = 36,000 rpm)

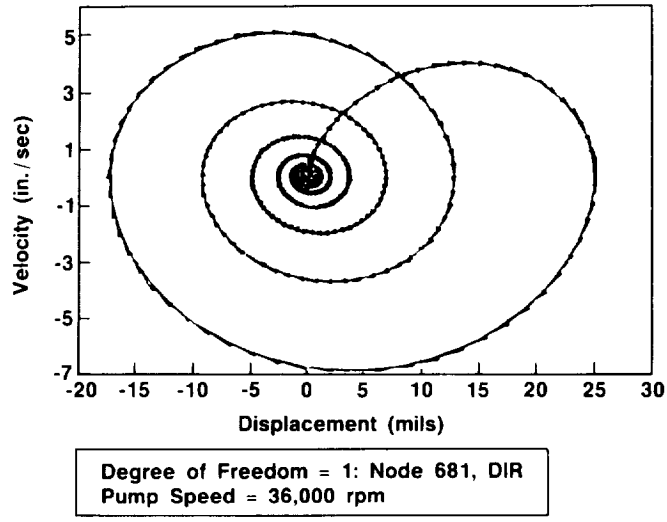

Fig. 6. State Space Representation of Blade Tip Motion

Since the blade is subjected to a periodic load, it is expected that certain forcing frequencies might excite a resonant condition. The frequency content of the forcing function is dependent upon the shaft speed and length of the contact arc; hence, there should be certain critical speeds and contact arcs at which the blade response is maximized. The existence of critical speeds is verified by the plots of steady-state rms blade tip displacement versus shaft speed presented in Fig. 7 through 9. The friction coefficient and magnitude of the normal load are identical in all cases, however, the contact arc varies from 10 to 30 degrees. In each graph, it is evident that extreme displacements occur at 29,500, 32,500, and 36,000 rpm. Thus, for each contact

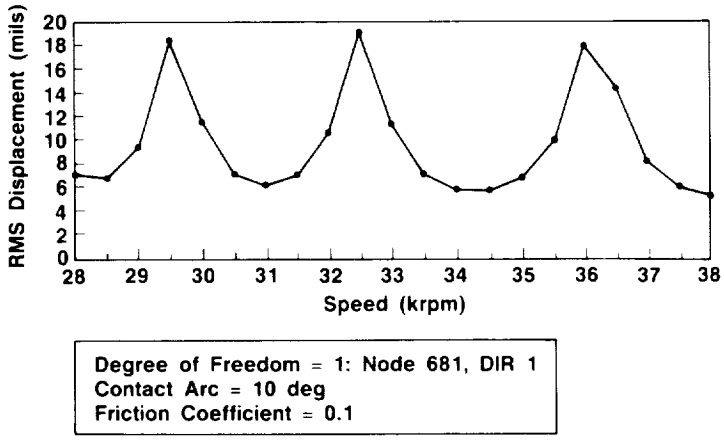

Fig. 7. Rms Blade Tip Displacement vs Speed (Contact Arc = 10 Deg)

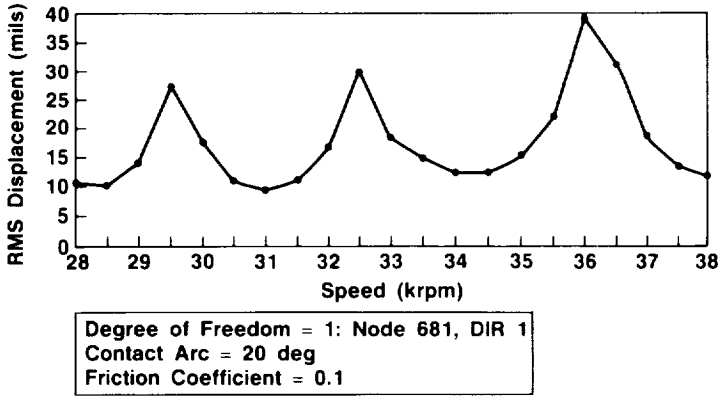

Fig. 8. Rms Blade Tip Displacement vs Speed (Contact Arc = 20 Deg)

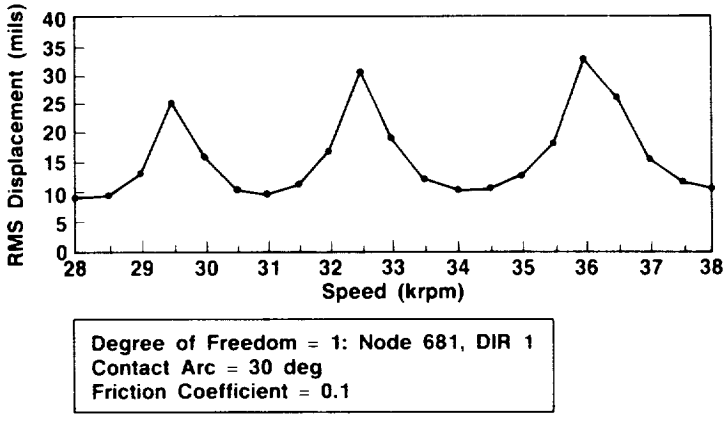

Fig. 9. Rms Blade Tip Displacement vs Speed (Contact Arc = 30 Deg)

arc, the blade response displays the same dependence on speed. Similarly, at a given speed, the amplitude of the response is dependent upon the contact arc. This suggests the existence not only of critical speeds but also of critical contact arcs, and provides motivation for further investigation into these observed patterns.

To explain the occurrence of the critical speeds, it is necessary to consider the frequency spectrum of the forcing function; recall that the time history of the forcing function was shown in Fig. 4 for one complete revolution of the shaft. Expressing the forcing function as a Fourier series and plotting the magnitude of the various Fourier coefficients as a function of harmonic number results in the plot of Fig. 10. The harmonic numbers should be interpreted as multiples of pump speed, thus the horizontal axis of Fig. 10 is actually a frequency axis. This representation of the force reveals a broad band of frequency content. Consequently, when the speed is such that the frequency of one force harmonic is equal to the frequency of a blade mode, then a resonant condition occurs. This is clearly presented in the Campbell diagram of Fig. 11, which indicates the speeds at which interferences occur between various harmonics of the forcing function and the first mode of the blade. Clearly, the ninth, tenth, and eleventh harmonics excite this mode at speeds of 36,000, 32,500, and 29,500 rpm, respectively. Therefore, the critical speeds are simply those at which a resonant condition exists between one harmonic of the forcing function and the first bending mode of the blade.

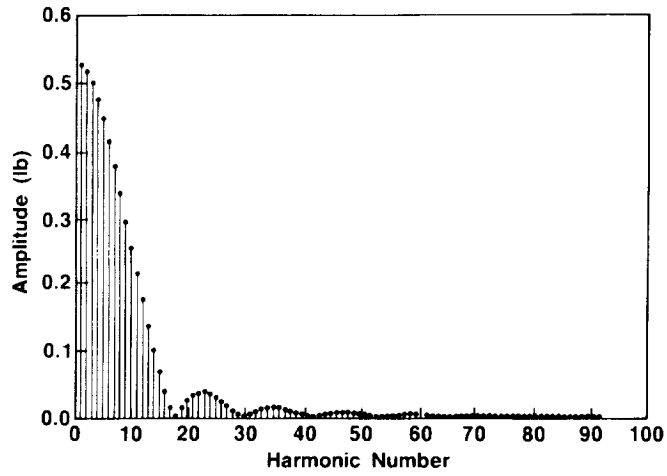

Fig. 10. Fourier Transform of Force (Half Sine Wave History Over Contact Arc Time Window = 1 Revolution)

Comparison of Fig. 7 through 9 indicates that although the dependence of the response on speed is identical in all three cases, the amplitude of the displacement varies with the contact arc. To investigate this observation, use the Fourier series representation of the forcing function and vary the length of the contact arc. Thus the magnitude of each harmonic may be expressed as a function of the contact

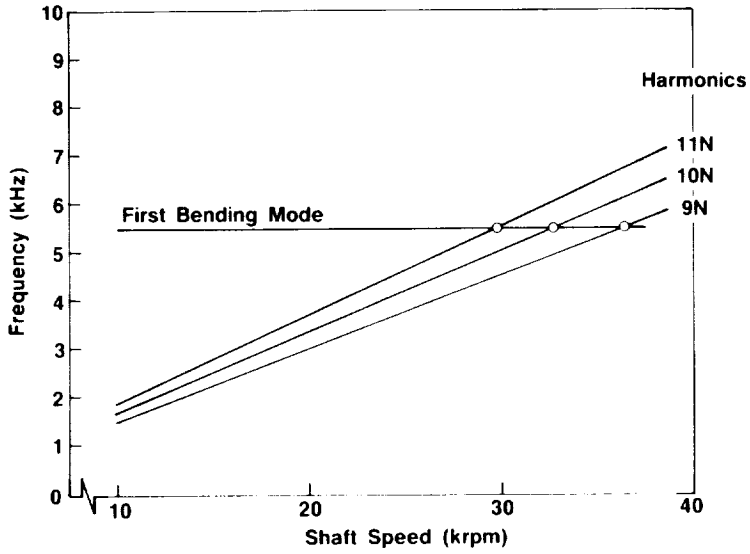

Fig. 11. HPFTP First-Stage Blade Campbell Diagram

arc as shown in Fig. 12; here only the ninth, tenth and eleventh harmonics are presented because they were identified as causing interferences within the operating range of the turbine. It is clear from the Fig. 12 that there is a unique angle for which each harmonic attains its maximum value. This explains the difference in blade response for different contact arcs at a given speed. The magnitude of each harmonic of the friction force is a function of the contact arc, therefore there is a specific contact arc that yields the greatest response at each critical speed. These combinations of speed and contact arc, which can be retrieved from Fig. 11 and 12, are listed in Table 2. It should be noted that the critical contact arcs are within the range of wear observed in the SSME first-stage tip seal.

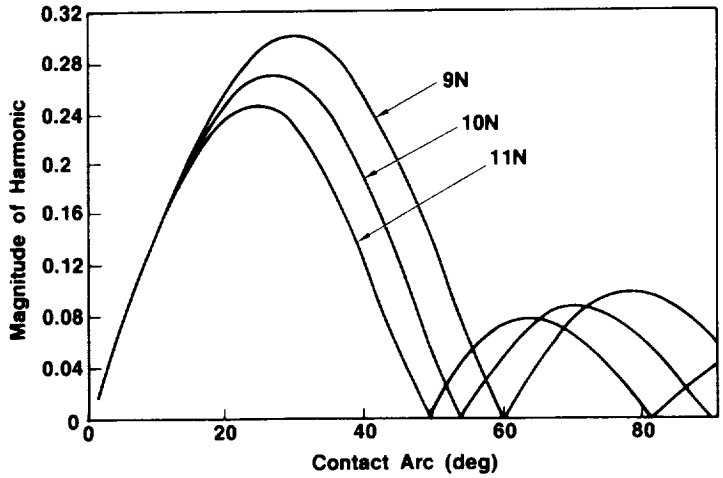

Fig. 12. Forcing Function Magnitude vs Contact Arc

Table 2. Critical Speed and Contact Arc Combinations

Resonant Harmonic	Critical Speed (rpm)	Critical Contact Arc (deg)
9	36,000	27.3
10	32,400	24.6
11	29,455	22.4

In addition to considering different speeds and contact arcs, the sensitivity of the response to the location of the applied load was also investigated. Separate response analyses were completed with the friction force applied at the airfoil tip near the leading edge, midchord, and trailing edge locations. A summary of the results are presented in Table 3, which shows that the highest stresses were found when forcing the blade at the trailing edge.

Table 3. Normalized Radial Stress at Shank Root (1 lb peak friction force)

Contact Arc (deg)	Force Applied	Steady State rms Stress (psi)		
		29,500 rpm	32,500 rpm	36,000 rpm
10	TE	128	129	125
10	MC	102	106	100
10	LE	97	101	94
20	TE	190	208	205
20	MC	148	170	167
20	LE	145	160	157
30	TE	170	206	220
30	MC	140	169	182
30	LE	130	158	170
NOTE: TE = trailing edge, MC = midchord, amd LE = leading edge				

The stresses presented in Table 3 have been normalized to show the blade response due to a a peak friction force of 1 pound. Using the maximum stress (220 psi) given in this table, it is easy to calculate the friction force necessary to create a given alternating stress. For example, an alternating stress of 5000 psi rms would require a peak friction force of 22.7 pounds. Assuming a coefficient of friction of 0.2 would translate this into 114 pounds of normal force, which is entirely within the expected range. Therefore, significant alternating stresses can be generated by blade tip rubbing.

In summary, the turbine blade parametric analysis provided several interesting results. The significant dependence of the maximum steady-state response upon both speed and contact arc is summarized by the surface shown in Fig. 13. This plot provides a qualitative representation of the effects of shaft speed and contact arc, and clearly illustrates the existence of critical conditions. The speed axis shows the frequency response of the blade, while the contact arc axis tells how the magnitude of the driving force varies. Critical speeds and/or contact arcs occur when these variables produce a maximum response as shown in Fig. 13.

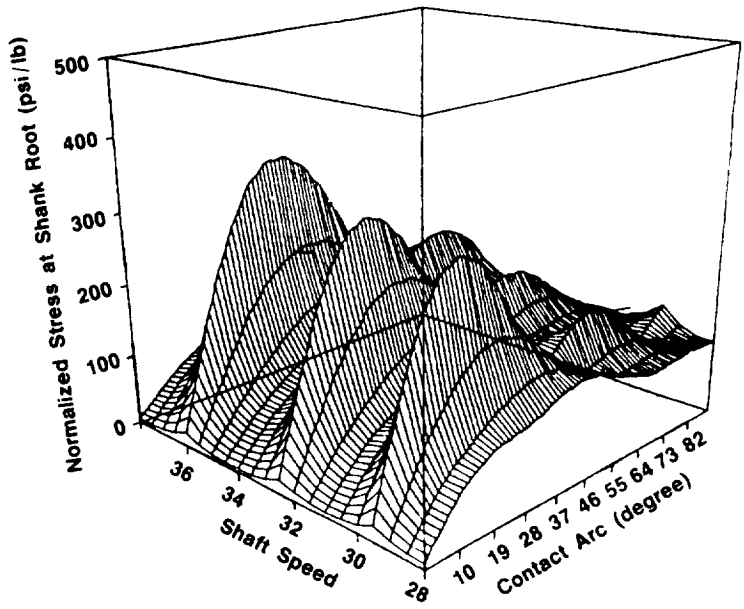

Fig. 13. Normalized Stress as a Function of Speed and Contact Arc

CONCLUSIONS

General conclusions, which can be drawn from the analysis, are that for a turbine blade under tip rubbing excitation, there exist distinct critical speeds at which the dynamic response of the blade is maximized. Furthermore, at each speed, a critical contact arc exists which maximizes the response of the blade. The overall maximum response occurs at the point where the critical speed and critical contact arc occur simulataneously.

The parametric analysis also provided information for specific conclusions regarding the SSME turbine blade. From the results of the analysis, three critical speeds were indentified within the range of operating speeds. These critical operating points represent the speed at which resonance occurs between the applied friction load and the first bending mode of the blade. In addition, three critical contact arcs that maximize the amplitudes of the resonant force harmonics were

identified within the range of observed wear in the SSME first-stage tip seal. Finally, the rms alternating stresses at the blade root were found to be significant depending upon the value and rub location of the friction force. No measurements of friction force have been made, however, the analysis shows that sizable stresses can be produced with reasonable values of friction force.

It is intended that the results of the linear parametric analysis presented herein will provide guidance in the preparation of the full-scale test program, and that the combination of analytical and empirical results will contribute to a fundamental understanding of the tip rubbing problem.